

Neutron-induced fission of the 26 min ^{235}U isomer

A. D'Eer and C. Wagemans

*Nuclear Research Center SCK/CEN, B-2400 Mol, Belgium
and State University, B-9000 Gent, Belgium*

M. Nève de Mévergnies

Nuclear Research Center SCK/CEN, B-2400 Mol, Belgium

F. Gönnerwein

Universität Tübingen, D-7400 Tübingen, Federal Republic of Germany

P. Geltenbort

Institut Laue-Langevin, F-38042 Grenoble, France

M. S. Moore

Los Alamos National Laboratory, New Mexico 87545

J. Pauwels

Joint Research Center, Commission of the European Communities, Central Bureau for Nuclear Measurements, Geel, Belgium

(Received 24 November 1987)

We have measured the neutron-induced-fission cross section of the ^{235}U isomer with cold and with thermal neutrons. Because of its short half-life (26 min), preparation of an adequate isomeric target is the major difficulty. A simple and easy-to-operate technique has been developed. The cross-section ratio of isomer to ground state is measured to be 1.61 ± 0.44 and 2.47 ± 0.45 for the cold and the thermal neutrons, respectively.

I. INTRODUCTION

^{235}U has an isomeric level ($\frac{1}{2}^+$) with a very low excitation energy of 76.8 ± 0.5 eV above the ground level ($\frac{7}{2}^-$). This metastable state $^{235}\text{U}^m$ decays with a half-life of 26 min to the ground state by means of a strongly internally converted $E3$ transition in which the emitted electrons originate from the outer atomic shells.¹⁻³

The study of the $^{235}\text{U}^m$ neutron-induced-fission reaction is interesting since it gives the possibility of comparing for a single nucleus the characteristics of the fission process for two states (ground and isomeric state), which are substantially different in structure (spin and parity), but which lead to practically identical excitation energies of the fissioning nucleus. It is also interesting for reactor physics and astrophysics because the isomeric state can be populated by inverse internal conversion.⁴ The major difficulty in studying the $^{235}\text{U}^m(n, f)$ reaction is the target preparation, mainly because the short half-life prevents the accumulation of a large quantity of isomeric nuclei on the targets.

II. TARGET PREPARATION

A. Requirements

In order to perform the fission measurement under clean conditions, the target must satisfy the following requirements.

(i) Sufficient amounts of isomeric nuclei have to be collected.

(ii) The target substrate must be as thin as possible to enable detection of both fission fragments in coincidence.

(iii) The target nuclei must strongly adhere to the substrate to avoid desorption under measuring conditions (i.e., vacuum for the present case).²

(iv) Contamination by ^{239}Pu and $^{235}\text{U}^g$ (i.e., other fissile species) must be low compared to $^{235}\text{U}^m$ and well known.

An easy-to-operate routine production system has to be installed close to the neutron irradiation facility, in order to minimize the time needed for manipulation and transport.

B. Survey of production methods

^{239}Pu has a 100% alpha decay with a half-life of 2.4×10^4 yr populating almost uniquely (> 99%) the isomeric level (Fig. 1).³ By conservation of energy and momentum, calculations give average kinetic energies for the alpha particle and the $^{235}\text{U}^m$ nucleus of 5.1 MeV and 88 keV, respectively. Due to electron shake-off the recoil nucleus has a positive charge. For heavy nuclei, these charge distributions lie almost exclusively in the range between 0 and +2 charge units.⁵

All production methods are based on the alpha decay of ^{239}Pu , namely:

(1) Chemical separation:^{6,8} involves a double extraction of ^{235}U from a plutonium solution. Efficient separation is

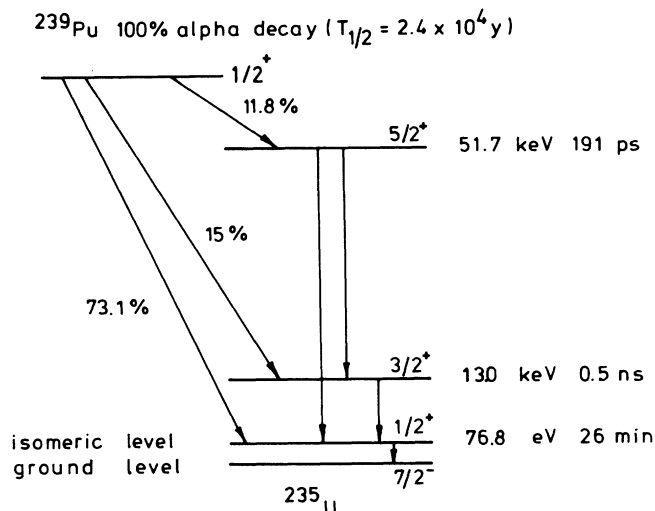


FIG. 1. Population of the ^{235}U lower levels by ^{239}Pu alpha decay (schematic).

usually arduous and time consuming, resulting in a low and sometimes unknown ratio of isomer to ground state. Large amounts of Pu may be handled, at least in principle.

(2) The gas jet transport system:^{7,8} is based on the adhesion of nuclei to aerosols. A gas, artificially enriched with aerosols, streams over plutonium layers and transports the recoil nuclei, with an 80% overall efficiency under optimized conditions.

(3) The stopping foil method:⁹ isomeric recoils, escaped from a plutonium layer and slowed down by collisions with gas atoms, are attracted to the conductive surface of a collector foil by means of an electric field.

C. The experimental setup

The stopping foil method was chosen, since it is a clean and easy-to-operate technique which allows the use of thin target substrates (see Fig. 2). The mother source¹⁰ was built in the form of a 40 cm diameter aluminum

sphere, internally coated with a highly enriched plutonium-trifluoride layer with a thickness of about $10 \mu\text{g cm}^{-2}$. The recoils are slowed down when traversing the air-filled space and are guided, by means of a high voltage, towards two polyimide foils ($25 \mu\text{g cm}^{-2}$) covered with a $30 \mu\text{g cm}^{-2}$ gold layer. The foils are placed in the center of the chamber. At the end of each collection, the foils are stuck together face to face. In this way a "sealed" target is obtained and possible desorption of the isomer during the fission experiment is avoided. The ^{235}U buildup on the foils was calculated as a function of collection time (t_c) and is shown in Fig. 3.

The ratio of isomer to ground state populations $N\{^{235}\text{U}^m\}/N\{^{235}\text{U}^g\}$ or shortly N_m/N_g is given by

$$\frac{N_m}{N_g} = \frac{1 - \exp(-\lambda t_c)}{\lambda t_c - 1 + \exp(-\lambda t_c)},$$

λ being the isomeric decay constant. It is obvious that while the amount of isomer increases with time up to its limit value, N_m/N_g decreases continuously. The compromise of a one half-life collection time was chosen with N_m equal to half of its limit value and

$$\frac{N_m}{N_g} = \frac{1}{2 \ln 2 - 1} = 2.59.$$

In assessing the efficiency of the collection method, the number of isomeric nuclei was determined by conversion electron detection using a channel electron multiplier.⁹

Alpha measurements of $^{235}\text{U}^m$ targets were performed to check for possible contamination. The alpha spectra (Fig. 4) showed a clear ^{239}Pu peak. Further analysis revealed the presence of ^{236}Pu and its daughter products.

The preparation of isomeric targets was optimized as a function of two parameters, gas pressure and high voltage, which are correlated by the process of electrical breakdown (Paschen's law). The optimum conditions were found to be 25 mPa for the pressure and 200 V for the high voltage, the catcher foil being negative with respect to the ^{239}Pu deposit.

The number of isomeric nuclei on the target at the end

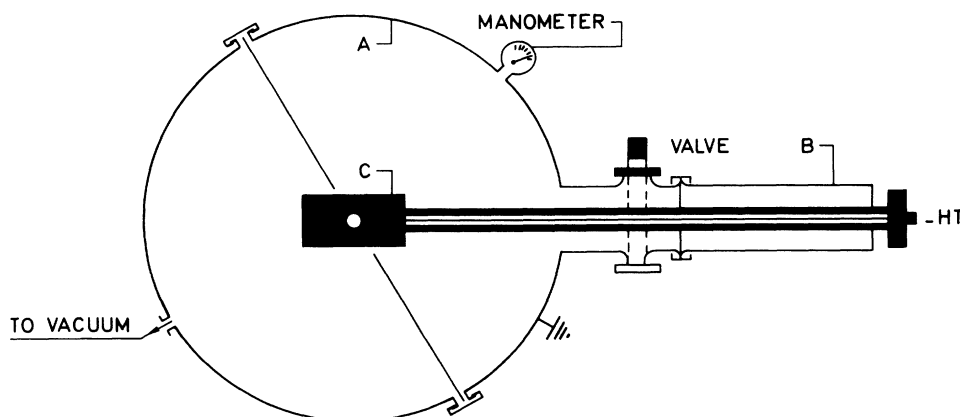


FIG. 2. Target preparation set-up. A: aluminum sphere ($\phi = 40 \text{ cm}$) with inner coating of $^{239}\text{PuF}_3$; B: lock chamber; C: sliding target holder.

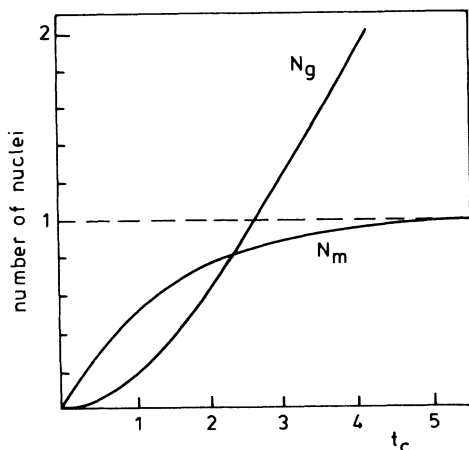


FIG. 3. Buildup of isomeric (N_m) and ground-state (N_g) ^{235}U nuclei on the target in units of 7×10^{10} nuclei as a function of the collection time t_c (in units of $T_{1/2} = 26$ min).

of the collection was measured to be $(6 \pm 3) \times 10^9$. The spread is due to a 50% overall reproducibility of the system. Important for the cross-section measurement is the average of 20% ^{239}Pu contamination of the $^{235}\text{U}^m$ targets. During the first experiment (with cold neutrons), the ^{239}Pu contamination was not measured routinely for every sample, so only the average level of contamination could be determined. In the second experiment (with thermal neutrons) the ^{239}Pu contamination was assessed sample by sample.

III. FISSION EXPERIMENT

The experiment was carried out at the High Flux Reactor of the Institut Laue-Langevin (Grenoble, France). The $^{235}\text{U}^m(n, f)$ reaction cross section was measured for two different neutron energies in the $1/v$ region.

A neutron beam with a peak energy of 5 meV in the wavelength representation of the Maxwellian flux and a flux of 1.5×10^9 neutrons $s^{-1} \text{cm}^{-2}$ (Ref. 11) was chosen for the first experiment (Fig. 5). Since it was carried out at the end of a 100 m long curved neutron guide, the

background conditions were excellent and no events to be confused with fission events could be detected. However, the data suffered from poor statistics and from some uncertainty in the ^{239}Pu contamination level.

A beam with an eight times higher flux (1.2×10^{10} neutrons $s^{-1} \text{cm}^{-2}$) (Ref. 11) and with a peak energy of 56 meV in the wavelength representation of the Maxwellian flux (Fig. 6) was used during the second experiment. It was available directly at a beam port in the reactor hall. Due to the very high neutron and gamma background, a well-collimated beam and heavy shielding (successive layers of B_4C , Pb, polyethylene) around the fission chamber were required.

The fission events are identified by coincident detection of both fragments, using two 30 cm^2 Canberra PIPS (passivated implanted planar silicon) detectors in a geometry with a calculated detection efficiency of $80 \pm 4\%$. This value was experimentally verified by inducing fission reactions in a known ^{235}U layer. The use of a coincidence circuit greatly facilitates the distinction between true fission events and noise. The information obtained, namely the pulse height of both fission fragments (PH1, PH2), is written on tape using a Canberra multiparameter system. The data are stored in list mode. An internal clock in the system produces a time mark on the tape every second.

IV. FISSION CROSS SECTION

A. Principles

Upon irradiating a freshly prepared target, the fission counting rate $c_f(t)$ can be expressed by

$$c_f(t) = a_i \exp(-\lambda t) + b_i + c_i \quad (1a)$$

with

$$a_i = \varepsilon \phi \sigma \{^{235}\text{U}^g\} \left[\frac{\sigma \{^{235}\text{U}^m\}}{\sigma \{^{235}\text{U}^g\}} - 1 \right] N_i \{^{235}\text{U}^m\}, \quad (1b)$$

$$b_i = \varepsilon \phi \sigma \{^{235}\text{U}^g\} (N_i \{^{235}\text{U}^m\} + N_i \{^{235}\text{U}^g\}), \quad (1c)$$

$$c_i = \varepsilon \phi \sigma \{^{239}\text{Pu}\} N_i \{^{239}\text{Pu}\}, \quad (1d)$$

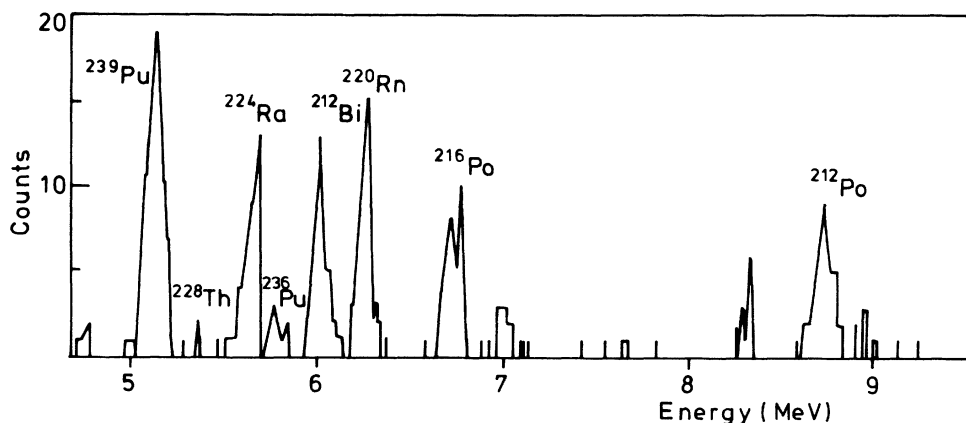


FIG. 4. Alpha spectrum of a $^{235}\text{U}^m$ target showing contamination by ^{239}Pu and by ^{236}Pu and its daughter products. The ^{236}Pu is present as an impurity in the basic ^{239}Pu material.

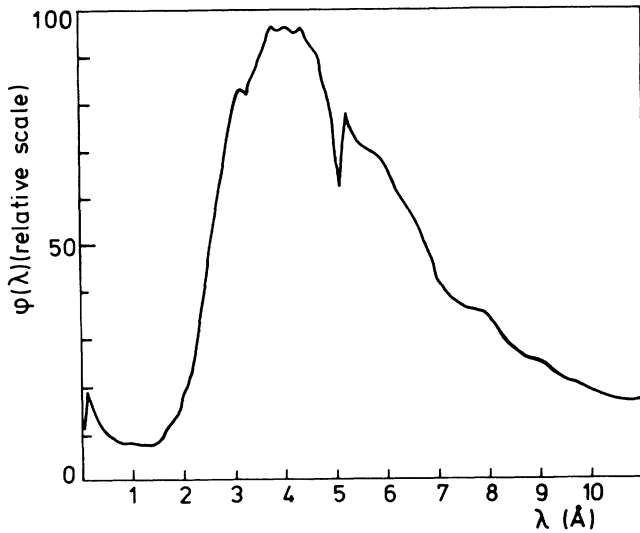


FIG. 5. Differential neutron flux as a function of neutron wave length, coming out of the neutron guide *H14* of the ILL High Flux Reactor (Ref. 11). Peak neutron energy is 5 meV.

where t is the time ($t=0$ at the end of target preparation), λ is the isomeric decay constant, ϵ is the detection efficiency ($=0.8$), ϕ is the neutron flux on the target (neutrons $\text{cm}^{-2}\text{s}^{-1}$), σ is the fission cross section (cm^2), N is the initial number of nuclei at the end of the collection, and i is the measuring cycle number.

The appearance of the expected counting rate $c_f(t)$ is plotted in Fig. 7 under different assumptions for the sign of a_i and, hence, for the cross-section ratio.

From the above relations (1b) and (1c), the cross-section ratio $\sigma\{^{235}\text{U}^m\}/\sigma\{^{235}\text{U}^g\}$ or, shortly, σ_m/σ_g is deduced to be

$$\frac{\sigma_m}{\sigma_g} = 1 + 2 \ln 2 \frac{a_i}{b_i} \quad (2)$$

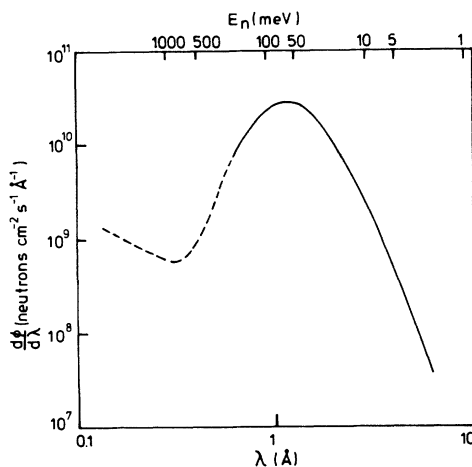


FIG. 6. Differential neutron flux as a function of neutron wave length, coming out of beam port *H12* of the ILL High Flux Reactor (Ref. 11). Peak neutron is 56 meV.

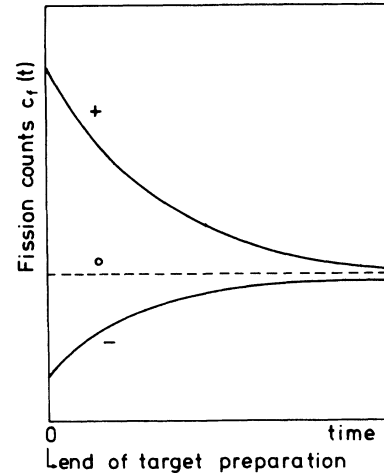


FIG. 7. Typical time evolution of the fission counting rate $C_f(t)$ under various hypotheses: $\sigma_m > \sigma_g$ (+ curve), $\sigma_m = \sigma_g$ (o curve), and $\sigma_m < \sigma_g$ (- curve).

for a collection time $t_c = T_{1/2}$. This expression is apparently independent of the ^{239}Pu contamination. However, since experimentally the sum of $b_i + c_i$ is obtained, the influence of the contamination is introduced when deducing c_i from the measured data. Under optimized conditions, a freshly prepared target contained the following typical quantities of ^{235}U and ^{239}Pu :

$$\begin{aligned} N_i\{^{235}\text{U}^m\} &= 6 \times 10^9 \text{ atoms} , \\ N_i\{^{235}\text{U}^g\} &= 2.3 \times 10^9 \text{ atoms} , \\ N_i\{^{239}\text{Pu}\} &= 1.6 \times 10^9 \text{ atoms} . \end{aligned}$$

B. Data analysis

Each experiment consisted of I cycles, each cycle i ($i = 1, \dots, I$) having the following sequence.

- (1) Target preparation: collection time $t_c = T_{1/2} = 26$ min.
- (2) Transport of the foil and positioning in the fission chamber: delay time t_d (typically 10 min).
- (3) Neutron induced fission measurement: measuring time t_m (typically 2 h).
- (4) Determination of the ^{239}Pu contamination by alpha counting, off line, after the fission counting was completed.

The sum of t_d and t_m is referred to as the decay time T .

For each cycle the time evolution of the fission counting rate is registered event by event. For I cycles the total number of counts expected theoretically during the time interval $(t, t + \Delta t)$ is given by the following integral, based on formula (1):

$$\int_t^{t+\Delta t} c_f(t) dt = A \exp(-\lambda t) + B + C \quad (3a)$$

for $t \geq t_d$, with

$$A = \frac{\sum_i a_i}{\lambda} [1 - \exp(-\lambda\Delta t)], \quad (3b)$$

$$B = \sum_i b_i \Delta t, \quad (3c)$$

$$C = \sum_i c_i \Delta t. \quad (3d)$$

Analogous to expression (2), the cross-section ratio is obtained when dividing (3b) by (3c):

$$\frac{\sigma_m}{\sigma_g} = 1 + 2 \ln 2 \frac{\lambda\Delta t}{[1 - \exp(-\lambda\Delta t)]} \frac{A}{B}. \quad (4)$$

For each experiment, the data can be transformed into an $I \times J$ two-dimensional matrix F . The number of fission counts in the matrix position (i, j) is represented by F_{ij} where i is the number of the cycle ($i = 1, \dots, J$), j is the number of the time interval $[(j-1)\Delta t, j\Delta t]$, ($j = 1, \dots, J$) with $J = T/\Delta t$.

In other words and according to (3a):

$$\sum_i F_{ij} = A \exp[-\lambda(j-1)\Delta t] + B + C. \quad (5)$$

A least-squares fit of the J data pairs $\{j, \sum_i F_{ij}\}$ with the predicted theoretical function $A \exp[-\lambda(j-1)\Delta t] + B + C$ would result in fitted values for the parameters A and $B + C$. However, it would be impossible to obtain a distinct value for B independent of C which is essential in the cross-section ratio determination. Therefore, the component C expressing the contribution of the ^{239}Pu fissions, has to be subtracted from both sides of relation (5) prior to the application of the fitting procedure. The cross-section ratio will consequently become dependent on the corrections made for the ^{239}Pu contamination on the target foils.

Alpha measurements of irradiated foils were performed in order to obtain the plutonium contamination level C , expressed by a second $I \times J$ two-dimensional matrix PF . Here PF_{ij} is the constant number of ^{239}Pu fission counts per time interval j and per target i . Subtracting the matrices F and PF results in a matrix UF containing only uranium fission counts.

Application of the least-squares fitting procedure to the J pairs

$$\{\exp[\lambda(j-1)\Delta t], \sum_i UF_{ij}\}$$

results in the parameter values $A(\text{fit})$, $B(\text{fit})$, together with their corresponding standard deviations. The quality of the fit is evaluated by means of the correlation coefficient r .

Finally, the cross-section ratio of the isomer to ground state $R = \sigma_m/\sigma_g$ is obtained by inserting the fitted parameter values in Eq. (4). The corresponding standard deviation is calculated as follows: The x coordinates $\exp[\lambda(j-1)\Delta t]$ are assumed to be known exactly since the time information of the fission event is precise. The standard deviations on the ordinates $\sigma(\sum_i UF_{ij})$ are given by

$$\sigma \left[\sum_i UF_{ij} \right] = \left[\sigma^2 \left[\sum_i F_{ij} \right] + \sigma^2 \left[\sum_i PF_{ij} \right] \right]^{1/2}.$$

These standard deviations are taken into account for the least-squares fitting procedure and yield the standard deviations $\sigma[A(\text{fit})]$ and $\sigma[B(\text{fit})]$. The standard deviation on the final result is given by

$$\sigma(R) = 2 \ln 2 \frac{\lambda\Delta t}{1 - \exp(-\lambda\Delta t)} \frac{A(\text{fit})}{B(\text{fit})} \times \left[\frac{\sigma^2[A(\text{fit})]}{A^2(\text{fit})} + \frac{\sigma^2[B(\text{fit})]}{B^2(\text{fit})} \right]^{1/2} \quad (6)$$

based on the propagation of errors.

C. Results

In order to exclude the possibility of taking into account "false" fission events, being the accidental coincidence of a fission fragment and a background event caused by neutrons or gammas, the sum of the coincident pulse heights of both ADC's was inspected.

1. Experiment 1 ("cold" neutrons)

For both detectors, a clean fission fragment pulse height spectrum was observed. This is shown in Fig. 8, which gives the sum of the pulse-height spectra of all 25 measuring cycles performed during this experiment. The data points are plotted in Fig. 9 together with the fitted curve which has a 0.5 correlation coefficient. The cross-section ratio and its standard deviation are calculated to be $\sigma_m/\sigma_g = 1.61 \pm 0.44$.

2. Experiment 2 ("thermal" neutrons)

During this experiment five measuring cycles were performed. For both detectors, a clearly separable fission fragment pulse-height spectrum was observed as shown in Fig. 10. The data points are plotted in Fig. 11 together with the fitted curve which has a 0.9 correlation coefficient. The cross-section ratio and its standard deviation are calculated to be $\sigma_m/\sigma_g = 2.47 \pm 0.45$.

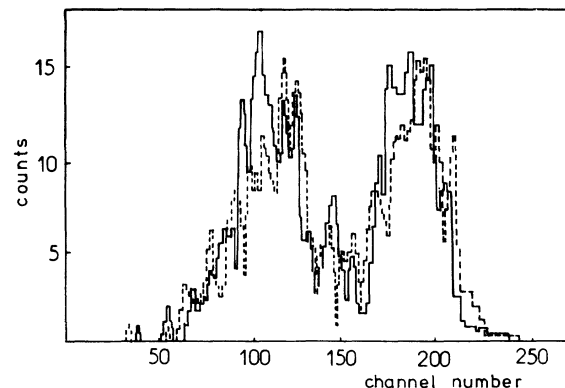


FIG. 8. Total pulse-height spectrum for experiment 1. Solid line: detector 1; dashed line: detector 2.

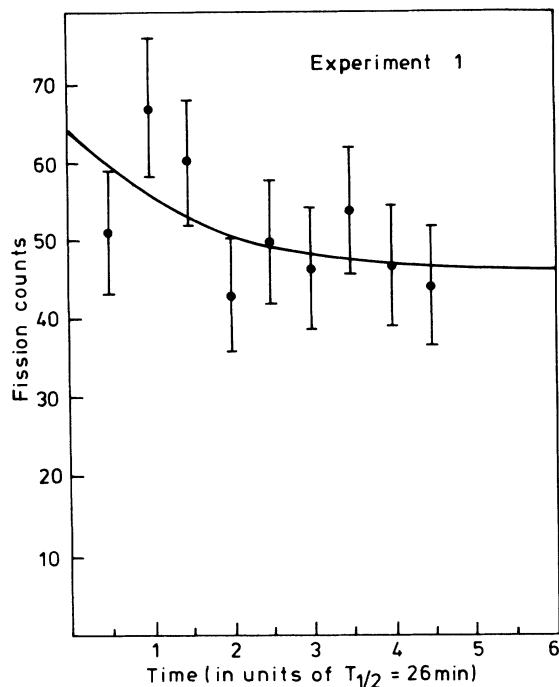


FIG. 9. ^{235}U fission counts per $0.5 T_{1/2}$ ($=13$ min) interval. The solid line represents the fitted curve with parameters $A = 18 \pm 13$, $B = 47 \pm 4$, and $r = 0.5$.

V. DISCUSSION

The present $^{235}\text{U}^m(n, f)$ measurements are the only ones obtained at fully characterized external neutron beams. This fact together with an adequate shielding of the detection chamber and coincident fission fragment detection resulted in clean background conditions. Our results suggest a possible energy dependence of σ_m/σ_g , which might indicate the presence of a strong low-energy resonance in the $^{235}\text{U}^m(n, f)$ cross section. However, the uncertainties on the results obtained with cold and with thermal neutrons are slightly overlapping, hence excluding a strong statement in this respect.

Recently, two other $^{235}\text{U}^m(n, f)$ experiments have been reported by Mostovoi and Ustroe¹² and by Talbert

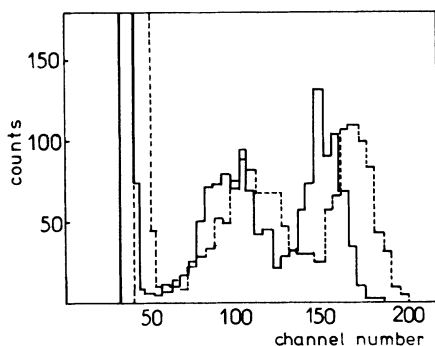


FIG. 10. Total pulse-height spectrum for experiment 2. Solid line: detector 1; dashed line: detector 2.

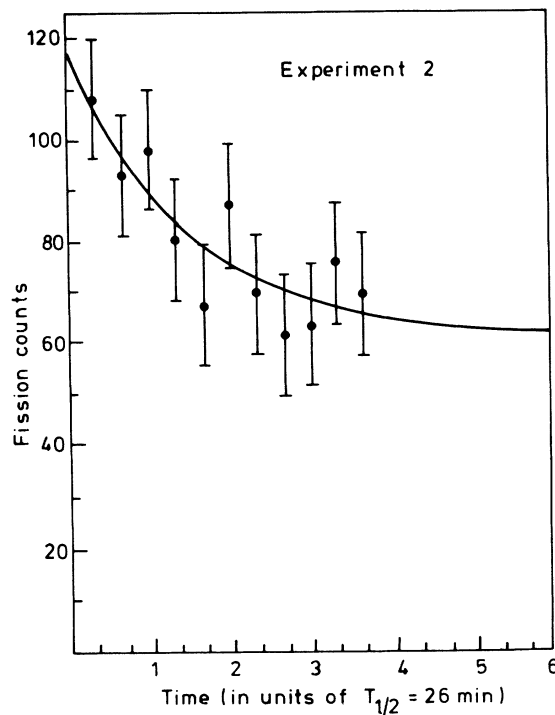


FIG. 11. ^{235}U fission counts per $\frac{1}{3} T_{1/2}$ (≈ 8.7 min) interval, starting at t_s . The solid line represents the fitted curve with parameters, $A = 58 \pm 16$, $B = 61 \pm 6$, and $r = 0.9$.

*et al.*⁸ In both cases, the neutron irradiation took place in a thermal reactor column. Mostovoi and Ustroe¹² prepared the $^{235}\text{U}^m$ layers in a very similar way as we did, i.e., using the stopping foil method.

Talbert *et al.*,⁸ on the other hand, applied a chemical separation technique. Despite the lack of complete information available on the spectral characteristics of the thermal neutron columns used in both experiments, these irradiation conditions are expected to be fairly comparable with our measurements using thermal neutrons. Our σ_m/σ_g value of 2.47 ± 0.45 is in good agreement with the value of 2.2 ± 0.4 reported by Mostovoi and Ustroe¹². It contradicts however the value of 1.42 ± 0.04 reported by Talbert *et al.*,⁸ which was obtained using a quite different target preparation technique. The reason for this discrepancy is not understood. All measurements confirm that $\sigma_m/\sigma_g > 1$.

Mostovoi and Ustroe¹² as well as Talbert *et al.*⁸ interpret this result as evidence that fission of $^{235}\text{U}^m$, induced by low-energy neutrons, proceeds predominantly by way of the 0^+ channel, which is clearly the lowest one. Such a conclusion is open to question, and depends on the detailed resonance properties of 0^+ and 1^+ resonances in $^{235}\text{U}^m + n$ at the neutron binding energy. Our best guess for the moment is that the 1^+ resonances for $^{235}\text{U}^m + n$ have the same properties as for $^{239}\text{Pu} + n$. We argue that this channel must be at least partially open in $^{235}\text{U}^m(n, f)$, because it has been observed in neutron induced fission of ^{237}U ,¹³ which by systematics should be less fissionable than $^{235}\text{U}^m$. If one calculates the probability of seeing fission through 0^+ and through 1^+ resonances at the level of 1.4–2.5 times that of $^{235}\text{U}^g$ with thermal

neutrons, one finds that, in the isolated resonance approximation, the probabilities are not very different. However, if there is a low-energy resonance that causes some change in the fission cross section ratio for cold and for thermal neutrons, such a resonance has a much higher probability of being 1^+ .

VI. CONCLUSION

The isomer to ground-state cross-section ratio has been measured with cold and with thermal neutrons. The results confirm that the neutron-induced-fission cross section of $^{235}\text{U}^m$ is larger than that of $^{235}\text{U}^g$. Our results also suggest the possible presence of a low-energy resonance in the $^{235}\text{U}^m (n, f)$ cross section.

ACKNOWLEDGMENTS

The authors thank with pleasure J. Van Audenhove and co-workers (Central Bureau for Nuclear Measurements Geel, Sample Preparation) for the supply of the exotic ^{239}Pu mother source. Special thanks are due to F. Van Velthoven, J. Brouwers, and J. Van Gils (Nuclear Research Center, Mol) for their help during the preparation of the experiments. Also the hospitality of the Institute Laue-Langevin (ILL), Genoble and the help of several of its staff members is gratefully acknowledged. In this respect we especially thank M. Belmonte, A. Billington, C. Middleton as well as the Radioprotection and Vacuum Groups. Last but not least, the Belgian National Fund for Scientific Research is acknowledged for its financial support.

-
- ¹V. Zhudov, A. Zelenkov, V. Kulakov, M. Mostovoi, and B. Odinov, *Pis'ma Zh. Eksp. Teor. Fiz.* **30**, 549 (1979) [*JETP Lett.* **30**, 516 (1979)].
- ²M. Nève de Mévergnies, *Vacuum* **22**, 463 (1972).
- ³M. Schmorak, *Nucl. Data Sheets* **40**, 1 (1983).
- ⁴V. Goldanskii and V. Namiot, *Sov. J. Nucl. Phys.* **33**, 169 (1981).
- ⁵K. Sevier, *Low Energy Electron Spectrometry* (Wiley Interscience, New York, 1972), p. 201.
- ⁶M. Nève de Mévergnies and P. del Marmol, *Phys. Lett.* **49B**, 428 (1974).

- ⁷H. Wollnik, *Nucl. Instrum. Methods* **139**, 311 (1976).
- ⁸M. Talbert, J. Starner, S. Balestrini, M. Attrep, D. Efurud, and F. Roensch, *Phys. Rev. C* **36**, 1896 (1987).
- ⁹M. Nève de Mévergnies, *Nucl. Instrum. Methods* **109**, 145 (1973).
- ¹⁰J. Pauwels, R. Eykens, A. D'Eer, M. Nève de Mévergnies, and C. Wagemans, *Nucl. Instrum. Methods* **A257**, 21 (1987).
- ¹¹P. Ageron (private communication).
- ¹²V. Mostovoi and G. Ustroev, *At. Energy* **57**, 141 (1984).
- ¹³J. McNally, J. Barnes, B. Dropesky, P. Seeger, and K. Wolfsberg, *Phys. Rev. C* **9**, 717 (1974).